# Chapter 18
# Ventilation System Analysis

## 18.1 Ventilation Design

*Purpose* The ventilation system influences the cockpit comfort conditions and removes battery-evolved gases and battery-heated air from the battery compartment at a specified minimum rate.

*Discussion Restrictions* There may be separate cockpit and battery ventilation subsystems. But we consider only the case in which each subsystem (or entire system) has one inlet and one outlet. This will keep the analysis for the flow through the system simple and focused on the basic ideas.

*Battery Ventilation* The race rules specify the minimum flow requirements for the battery compartment. Chapter 16 gives this requirement as a fan-forced flow of at least 280 L/min. This flow must be present whenever the battery is connected to the main bus, and it must exhaust to the exterior of the car. The designer's task then is to insure that this flow is present under the most limiting condition. This will occur when the car is stationary and the battery fan, or fans, must supply the flow unaided by the motion of the car.

*Driver Comfort* Figure 18.1 shows the summer human *comfort zone* (adapted from ASHRAE (1981)) defined by lines of constant temperature *(T)* and relative humidity *(Φ)*.

We would like the cockpit conditions to remain within this zone. But if the outside air temperature is typical of a late June day, say an air temperature (*dry bulb* temperature) of 30 °C and relative humidity of 70 %, the figure shows that this cannot be done without air conditioning. The weight and power penalties that accompany air conditioning preclude its use in solar racers

Therefore, the temperature and humidity of the air entering the cockpit will be those of the outside air. Our objectives then become to prevent the air temperature in the cockpit from exceeding that of the outside air and to minimize the direct heating of the driver by solar radiation.



E. F. Thacher, *A Solar Car Primer,* DOI 10.1007/978-3-319-17494-5_18

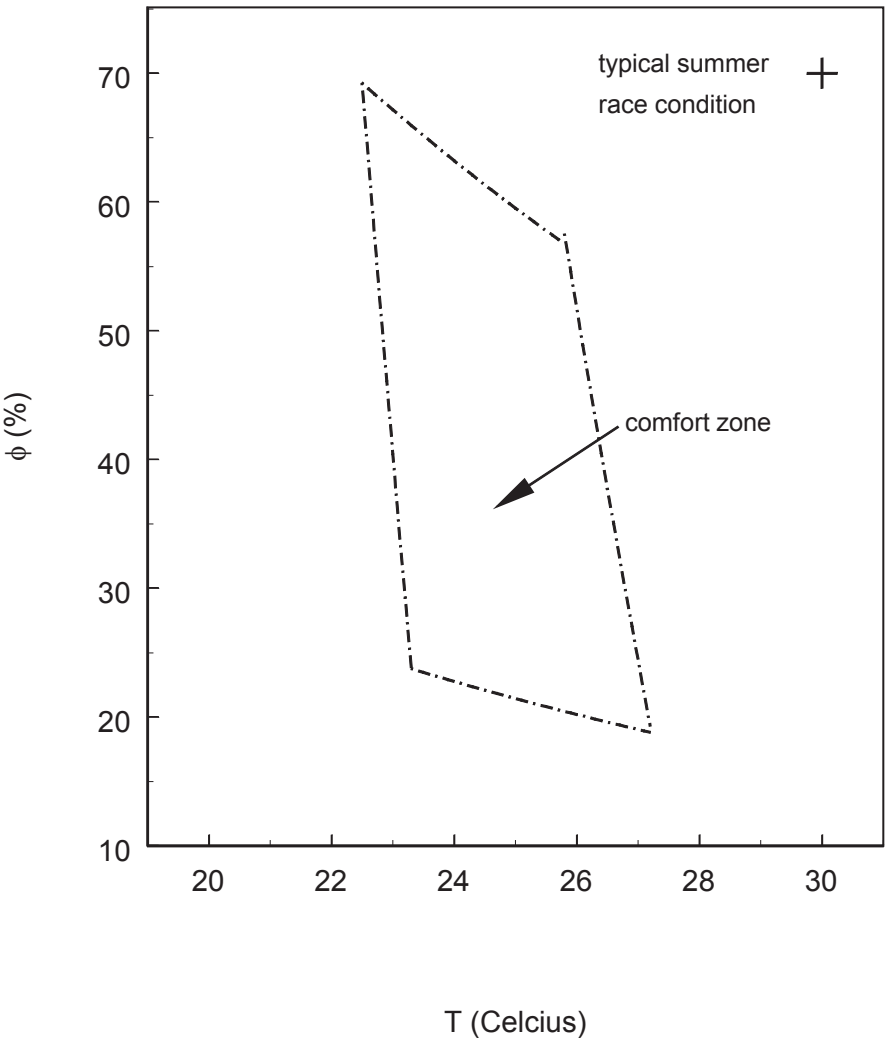


**Fig. 18.1** ASHRAE summer comfort zone

The options available are: reducing the solar gain through the canopy, reducing the absorption of solar radiation by surfaces in the cockpit, and changing the air in the cockpit. The latter can be done by providing forced circulation of outside air through the cockpit. Making the cockpit surfaces more reflective reduces absorption. The former can be done by shading, tinting or coating the glazing, and reducing the amount of glazing, subject to meet the visibility requirements of the race rules and to provide sufficient light to read the instruments.

*Analysis Outline* We would like to know the static pressure at the inlet and outlet of the ventilation system so that the ventilation drag and the ventilation drag coefficient

can be calculated. We would also like to know the flow through the battery box, to see if it is sufficient, and the temperature in the cockpit, to see if we might be in danger of frying the driver.

The first problem we will consider, then, is how to get an approximate pressure distribution around the car. This will be followed by an explanation of how to calculate the flow through the ventilation system, once the pressure at its inlet and outlet is known. Finally, a method for estimating the cockpit temperature will be explained. An example of each of these calculations is in Chap. 10.

## 18.2 Inlet and Exit Pressures

*Inlet and Outlet Locations* The pressure distribution in the external flow is a function of the vehicle's shape (see the list of assumptions below). This flow is approximately frictionless and therefore, may be analyzed by Bernoulli's equation. Thus if the velocity at a point in the flow can be found, then the static pressure at that point can also be found.

Bear in mind that the above statements do not apply to regions of separated flow. Also, near the inlet or outlet, the flow is deflected inward or outward, respectively, and this alters the static pressure at that point because the "shape" of the car at that point is effectively changed. For example, suppose an inlet for cockpit air is installed just ahead of the canopy. Some flow enters the car, so there is more flow just upstream of the inlet than just downstream of it. Velocities upstream of the inlet are therefore higher and the pressure is lower. Figure 18.2, adapted from Wallis (1971), illustrates this situation. Wallis observed that at a particular vehicle speed, the average inlet static pressure remains constant for any inlet flow, even though the pressures upstream and downstream of the inlet shift, as previously described, as the inlet flow changes.

Locating inlets at or near stagnation points will not only maximize flow but may also increase drag. Figure 18.2 shows an inlet near the stagnation point in front of the canopy. However, wind tunnel measurements of ventilation flow have shown that if the inlet is small and is located at the stagnation point in the nose of a highly streamlined car, the ram flow may be sharply reduced by small pitch changes which shift the stagnation point away from the opening. Wallis (1971) recommends placing a small outlet in a region where $p-p_\infty$ is negative or a large, low-loss outlet where $p-p_\infty$ is zero or slightly positive.

*Approximate Pressure Distribution* We now describe a simple method for estimating the pressures at the ventilation inlet and outlet using Bernoulli's equation. However, some idealizations must be made. These are:

1. The air outside the boundary layer behaves as if it had no viscosity.
2. The thickness of the boundary layer may be neglected.
3. There is no heat transfer to the air.

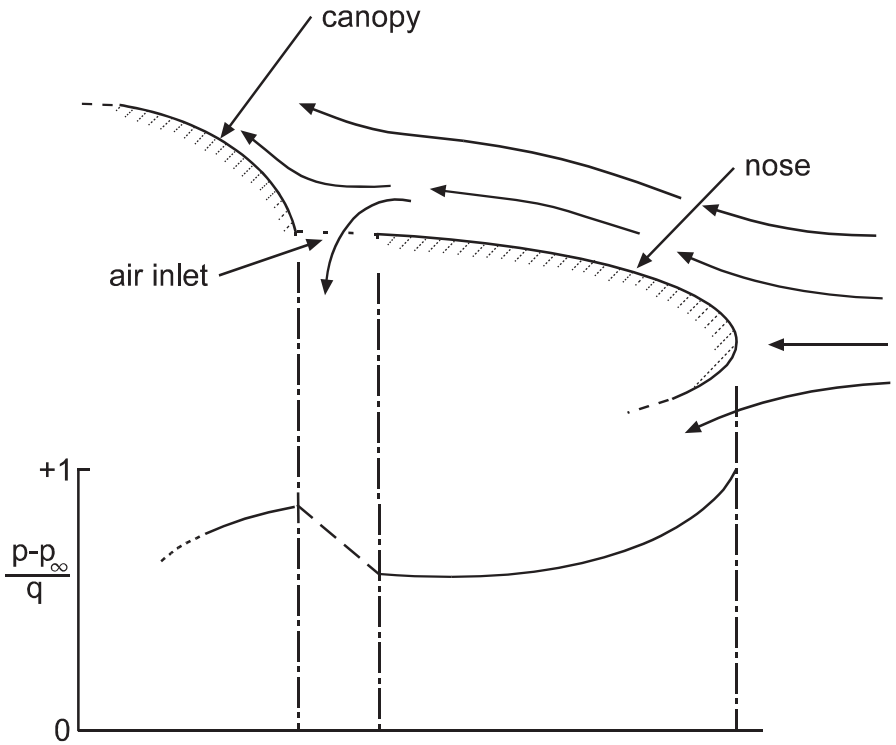


**Fig. 18.2** Qualitative pressure distribution

4. There are no regions of separated flow in the area of the car's surface that is of interest.
5. The flow is steady.
6. The flow about one car length upstream and downstream of the car is uniform.
7. The velocity distribution transverse to the vertical plane through the car's longitudinal axis is uniform.
8. The air density is constant.

The fundamental assumption of boundary layer theory is that viscous effects may be thought of as residing solely in the boundary layer. This implies assumption 1. Assumptions 1, 3, and 4 greatly simplify the description of the flow external to the boundary layer, allowing Bernoulli's equation to be used.

The boundary layer thickness is small compared to the dimensions of the car. The average error introduced by assumption 2 will be small. The boundary layer thickens as the flow moves toward the rear of the car, thus deflecting the stream surfaces away from the surface of the car. This displacement causes the velocity estimate near the car to be lower than the real flow. Therefore, by Bernoulli's equation, the pressure estimate will be higher than in the real flow.

Assumption 5 further simplifies the problem by removing time dependence from the variables. Assumption 6 allows the inlet and outlet properties of the flow to be calculated.

Assumption 7 relies on the observations that, in view of assumption 6, the flow is symmetric with respect to the car's centerline and, near the centerline, the transverse slope of the surface is usually small. Assumption 7, therefore, allows the flow to be approximated as two-dimensional (2D). That is, to be treated as if the velocity depended only on the coordinates perpendicular and parallel to the car's long axis.

The air density has been taken as approximately constant. This assumption will be used throughout this chapter. The error it introduces is small, but the simplification it allows is large.

Imagine the car placed in a 2D wind tunnel (H, height, and length, x, only: no flow perpendicular to the plane defined by H and x) that supplies the uniform upstream flow. A rule of thumb used in designing actual wind tunnels is that the tunnel cross-sectional area should be at least five times the profile area of the car. This makes the blockage effect that arises when the flow is confined between the car and the tunnel walls negligible. The tunnel is of width W and height H. But because the flow is 2D, W may be set to unity. Therefore the height, H, of the tunnel must be such that

$$H \times 1 \geq 5A_D \tag{18.1}$$

Because there are no boundary layers and no flow separation, the tunnel walls and the car's surface are stream surfaces. Using this fact and the known entrance and the exit conditions, we can sketch a plot of the stream surfaces (or streamlines in our 2D representation). From this information we can estimate the pressure distribution.

*Flow Net* A *flow net* is a net of streamlines and intersecting lines, called constant *velocity potential* lines. The flow net is constructed such that the streamlines and the lines intersecting them form, approximately, curvilinear squares. This means that the lines intersect at right angles and the sides of the figure thus constructed are approximately equal, as Fig. 18.3 shows.

First, the car is carefully drawn on crosshatched paper. Then the flow net is drawn by trial-and-error. The smaller the squares, the more accurate the approxima-

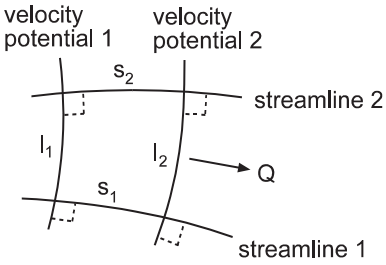


**Fig. 18.3** Curvilinear square

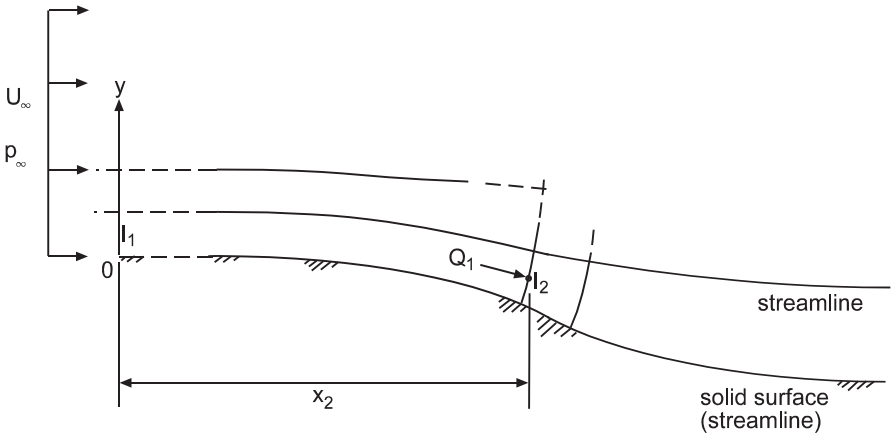


**Fig. 18.4** Partial flow net near a surface

tion. Figure 18.4 shows a streamline next to a surface and a curvilinear square with the center of its upstream side at a distance $x_2$ from the origin. We wish to estimate the pressure at this position.

Because of assumptions 1, 3, 4, 5, and 6, Bernoulli's equation is a constant throughout the flow. Therefore

$$p_\infty + \frac{1}{2}\rho U_\infty^2 = p_2 + \frac{1}{2}\rho V_2^2 \tag{18.2}$$

We solve Eq. (18.2) for the pressure difference $p_2 - p_\infty$ and divide by the dynamic pressure at the origin, $q_\infty$. This quotient is called the pressure coefficient, $c_P$.

$$c_{P_2} = 1 - \frac{V_2^2}{U_\infty^2} \tag{18.3}$$

The flow has a unit depth into the page, and so we may substitute

$$V_2 = \frac{Q_1}{l_2}, \quad U_\infty = \frac{Q_1}{l_1} \tag{18.4}$$

in Eq. (18.3). Note that the first of Eq. (18.4) gives the *average* velocity between the streamlines. As the flow net is made finer, this average approaches the true, ideal-flow velocity. The substitution produces

$$c_{P_2} = 1 - \frac{l_1^2}{l_2^2} \tag{18.5}$$

after canceling common factors. Measurement of $l_1$ and $l_2$ from the flow network gives the pressure coefficient. Measurement of the lengths, which are curved, by a ruler, which is straight, will only be approximate. However, this approximate measurement is consistent with the approximation to $V_2$ just discussed.

The pressure at point 2 is then

$$p_2 = p_\infty + c_{P_2} q_\infty \tag{18.6}$$

*Flow Around a Car* Fig. 18.5 shows a vehicle body in a 2D flow. (Some of the features that make the actual flow three-dimensional (3D), such as the wheels, are shown in dashed lines.) Note that unlike the flow in Fig. 18.4, the air must flow on both sides of the body.

The flow between the streamline at height $l_1$, $Q_1$ must divide at the front stagnation point such that

$$Q_1 = Q_U + Q_L = U_\infty l_1 \tag{18.7}$$

The previous method cannot be applied unless $Q_U$ and $Q_L$ are known. One way of estimating them would be to locate the stagnation streamline. The streamline should bisect the angle between the velocity potential lines labeled "$l_{1U}$" and "$l_{1L}$." In Fig. 18.5, the streamlines were drawn such that $Q_U \approx Q_L$.

A more analytical approach, which could be used as a check on the flow net near the car, is as follows. Locations 1 and 2 are imagined to be at pressures $p_1$ and $p_2$, respectively, and each to be "at" the point of flow division. Applying the Bernoulli equation to the flow along the upper surface of the car gives

$$p_2 - p_1 = \frac{1}{2}\rho(V_{1U}^2 - V_{2U}^2) \tag{18.8}$$

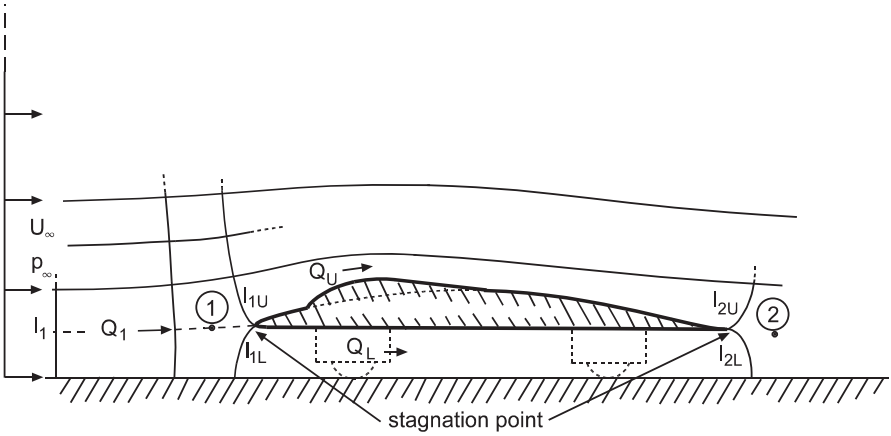


**Fig. 18.5** Divided flow

Applying Eq. (18.4) at each end of the surface gives

$$p_2 - p_1 = \frac{1}{2}\rho\left(\frac{1}{l_{1U}^2} - \frac{1}{l_{2U}^2}\right)Q_U^2 \tag{18.9}$$

The same procedure is now applied to the lower surface and the pressure changes are equated, giving

$$Q_U = \left(\frac{k_L}{k_U}\right)^{\frac{1}{2}} Q_L \tag{18.10}$$

where $k_L$ and $k_U$ are defined as

$$k_L = \frac{1}{2}\rho\left(\frac{1}{l_{1L}^2} - \frac{1}{l_{2L}^2}\right) \tag{18.11}$$

$$k_U = \frac{1}{2}\rho\left(\frac{1}{l_{1U}^2} - \frac{1}{l_{2U}^2}\right) \tag{18.12}$$

Using Eq. (18.10) with Eqs. (18.11) and (18.12) gives

$$Q_L = \frac{1}{\left(\frac{k_L}{k_U}\right)^{\frac{1}{2}} + 1} Q_1 \tag{18.13}$$

$$Q_U = \frac{1}{\left(\frac{k_U}{k_L}\right)^{\frac{1}{2}} + 1} Q_1 \tag{18.14}$$

Note that these relations require the flow net to be drawn such that

$$\frac{k_L}{k_U} > 0 \tag{18.15}$$

Therefore, $k_L$ and $k_U$ both must be positive or negative.

## 18.3 Design Strategy

*Design Operating States* The vehicle operational states that factors controlling the ventilation design are zero speed operation and the cruise condition. In the former state, drag is zero but so is the ram flow. The latter state not only causes the most

drag but can also provide the most ram flow. Therefore, the design strategy will be to locate the inlet and outlet, and design the ducting to minimize ventilation drag at the cruise condition and to size the fan, or fans, to provide the minimum required flows at zero speed.

Equation 2.8, repeated below as Equation (18.16), shows that the ventilation drag is the sum of the pressure force difference and the reaction force from the momentum change. Subscripts 1 and 2 denote the inlet and outlet, respectively. The subscript "x" denotes the component of the force or air speed parallel to the direction of motion. The bar over the gauge pressure symbol, $p_G$, denotes the average over the inlet or outlet. The symbol "A" denotes the area of the opening normal to the entering flow or pressure. If there is more than one subsystem, the drag contribution of each one must be calculated using Eqn (18.16). The total ventilation drag will be the sum of the subsystem drags.

$$D_V = (\overline{p}_{G1} A_1)_X - (\overline{p}_{G2} A_2)_X + \dot{m}_1 (V_{1X} - V_{2X}) \tag{18.16}$$

As for flow between streamlines, the cross-sectional area and speed for a given steady, constant-density flow in a duct (no leakage) are related by

$$Q = A_1 V_1 = A_2 V_2 = constant \tag{18.17}$$

The subscripts refer to any two stations in the flow path, and Q is the volumetric flow rate ($m^3/s$). The mass flow rate (kg/s) is

$$\dot{m} = \rho Q \tag{18.18}$$

## 18.4 Component Pressure Losses

The energy used to force the flow through components such as inlets, lengths of duct, sudden expansions and contractions, and valves causes a pressure drop in the flow direction. The net pressure drop (i.e., including pressure increases caused by fans) through the ventilation system must be equal to that imposed by the external flow. If this flow is zero, then the pressure rise caused by the fans must exactly cancel the total pressure loss at the desired internal flow.

The pressure loss in a component may be expressed by the product of a *head loss coefficient*, K, and a reference kinetic energy per unit mass.

$$h_L = \frac{\Delta p}{\rho g} = K_{12} \frac{V_{ref}^2}{2g} \tag{18.19}$$

The pressure loss would then be $\rho g h_L$ ($N/m^2$). The location of the reference kinetic energy will be identified for each loss coefficient case presented below.

The units of $\Delta p/\rho$ are $N \cdot m/kg$, or J/kg. This quotient represents the work per unit mass of air necessary to drive the flow through the component. Division by g, the acceleration of gravity, converts the units to meters. The power, or the rate of doing this work, would be

$$\dot{W} = \dot{m}\frac{\Delta p}{\rho} = \dot{m}gh_L \tag{18.20}$$

The head loss coefficients of the components are approximately independent of Reynolds number, that is, independent of the speed of the internal flow, as long as the flow is fully turbulent. However, in the case of components such as the cockpit or the battery box, the flow cross-sectional area is much larger than in the ducting connecting them, so the reference flow speed will be smaller. We must be sure to check the Reynolds number in such components.

We begin a flow calculation by assuming that the flow is turbulent and that the Reynolds number at each component is within the limits associated with the loss coefficient data for that component. The flow-dependent loss coefficients for the next iteration would be estimated from the flow just calculated. This procedure would be continued until the changes in the flow from the previous calculation are satisfactorily small.

*Coefficient Sources* Handbooks such as Idel'chik (1966) and Crane (1969) present information on loss coefficients for many different devices. Textbooks such as White (1986) also contain such information, but for a smaller variety of devices. The loss coefficient cases presented below may be found in any of these references. The loss coefficient curve for each component has been fitted with an interpolation formula.

*Rounded Inlet from Reservoir* Suppose the flow enters a pipe from an approximately infinite reservoir, such as the atmosphere, energy is lost from the flow at the entrance. This loss can be reduced by rounding the edge of the entrance. Figure 18.6 shows how $K_{12}$ for the rounded inlet changes as a function of the rounding radius. $V_{ref}$ is $V_2$, the velocity at the exit of the inlet. The equation for Fig. 18.6 is

$$K_{12} = a_0 e^{a_1\frac{r}{d} + a_2\left(\frac{r}{d}\right)^2 + a_3\left(\frac{r}{d}\right)^3 + a_4\left(\frac{r}{d}\right)^4} \tag{18.21}$$

where $r$ is the rounding radius, and $d$ is exit diameter. Table 18.1 gives the constants.

*Any Exit to a Reservoir* Because all the kinetic energy of the flow is lost by dissipation into the reservoir,

$$K_{12} = 1.0 \tag{18.22}$$

*Sudden Expansion and Contraction* When the flow from a duct enters a larger duct through an abrupt transition, that is, no gradually sloping duct connecting the two

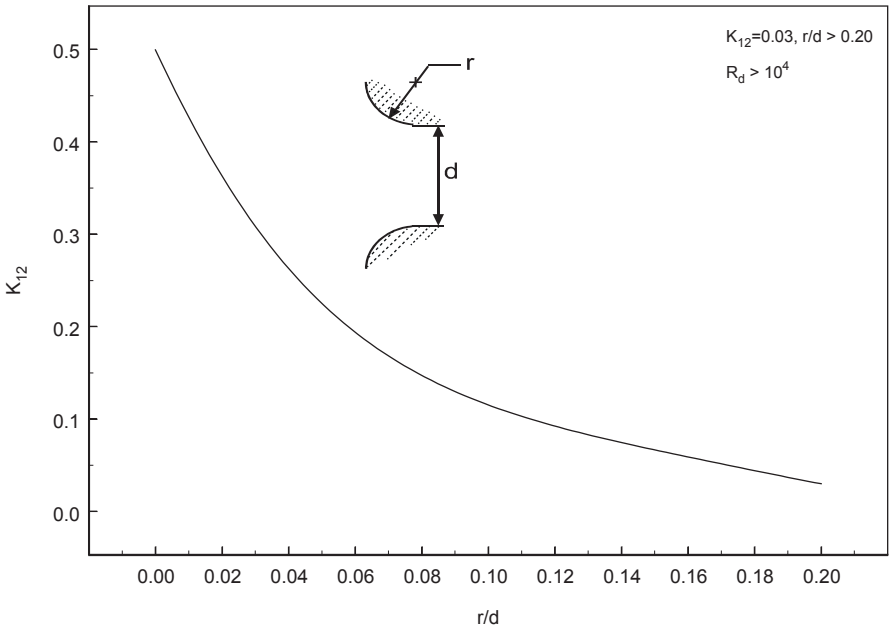


**Fig. 18.6** Rounded inlet loss coefficient

**Table 18.1** Constants for Eq. (18.21)

| $a_0$ | $a_1$ | $a_2$ | $a_3$ | $a_4$ |
|---|---|---|---|---|
| 0.499540 | −15.415485 | −40.244830 | 721.990759 | −2432.856432 |

conduits, energy is lost in the sudden expansion. When the flow leaves a larger duct and abruptly enters a smaller, energy is lost in the sudden contraction. The reference velocity in both cases is that in the smaller pipe, denoted by the subscript "1."

The loss coefficient for the sudden expansion is

$$K_{12} = \left(1 - \frac{d_1^2}{d_2^2}\right) \tag{18.23}$$

and for the sudden contraction is

$$K_{12} = 0.42\left(1 - \frac{d_1^2}{d_2^2}\right) \tag{18.24}$$

*Diffuser* A diffuser is a conical-shaped duct that widens in the flow direction. Its purpose is to slow the flow and thus increase the static pressure. Figure 18.7 shows a diffuser and its associated loss coefficient. Note the minimum loss coefficient at a cone angle of about 5°. Below this angle, the length of the diffuser becomes

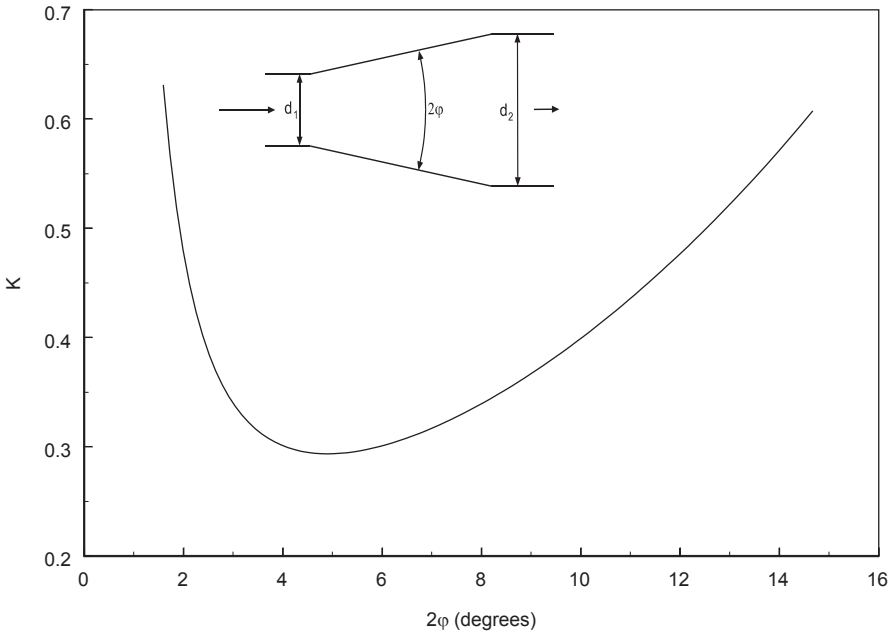


**Fig. 18.7** Diffuser loss coefficient

extreme and frictional losses increase. Above this angle flow separation occurs, beginning near the discharge end. As the cone angle increases the separation loss likewise increases until at about 40° the loss coefficient exceeds that of the sudden expansion.

The loss coefficient curve presented is for the so-called fully-developed[1] entrance flow. In this condition, the developing boundary layer inside the pipe has thickened until it reached the centerline of the pipe. This inlet condition yields the largest loss coefficient at a particular cone angle.

The diffuser pressure recovery coefficient, $c_P$, is the dimensionless pressure increase.

$$c_P = \frac{p_2 - p_1}{q_1} \tag{18.25}$$

The pressure and loss coefficients are related by

$$c_P = 1 - \frac{d_1^4}{d_2^4} - K_{12} \tag{18.26}$$

[1] If an initially uniform flow enters a duct, the boundary layer begins to thicken, just as on a flat plate.Eventually, it meets itself at the centerline.After that, the velocity profile no longer depends on the distance down the duct, but only on the radius from the centerline. Thus it is called *fully-developed*.

**Table 18.2** Diffuser constants

| $a_0$ | $a_1$ | $a_2$ |
|---|---|---|
| 1.359836 | −1.926919 | 0.605670 |

The equation of the loss coefficient curve is

$$K_{12} = a_0 (2\varphi)^{a_1 \ln(2\varphi) + a_2 \ln(4\varphi^2)} \tag{18.27}$$

Table 18.2 gives the constants for Eq. (18.27).

*Pipe, Tubing, and Ducting* The loss coefficient of duct, pipe, and tubing is

$$K_{12} = \frac{f L_{12}}{d} \tag{18.28}$$

where *f* is the *friction factor*. The friction factor depends upon whether the flow is laminar or turbulent and how rough the surface of the duct is.

The roughness is measured by the *relative roughness*, e/d, (or d/e as in Chap. 17) where *e* is the mean height of the bumps and *d* is the pipe's inside diameter. The roughness of commercial steel pipe is about 0.046 mm. Three-inch, schedule 40 pipe has an actual inside diameter of 3.068 in. or 77.95 mm. The relative roughness of this pipe would then be 0.00059. When the flow is turbulent, the loss coefficient increases with the relative roughness. However, when the flow is laminar, the roughness plays no role in the friction factor.

Figure 18.8 shows how the friction factor depends on e/d and the Reynolds number.[2] Laminar flow ends at Rd≈2300 and a transition region begins; the flow is fully turbulent by Rd≈4000. Note that in much of the turbulent region the friction factor is nearly independent of Rd, except for very smooth surfaces, whereas in the laminar region it varies inversely with Rd. Note the similarity in this respect between internal pipe flow and flow over a flat plate (Chap. 17). There are no reliable friction factors in the transition region.

In the case of a noncircular duct use the *hydraulic diameter*, $d_h$, defined as

$$d_h = \frac{4A_F}{P_W} \tag{18.29}$$

where $A_F$ is the cross-sectional flow area, and $P_W$ is the wetted perimeter of the duct. This approximation gives "reasonable accuracy," according to White (1986), who recommends the use of $2d_h/3$ for "extreme accuracy."

The friction factor in Fig. 18.8 is given by

[2] This is a simplified *Moody Chart*, named after L.F. Moody, who published a more elaborate chart in 1944.

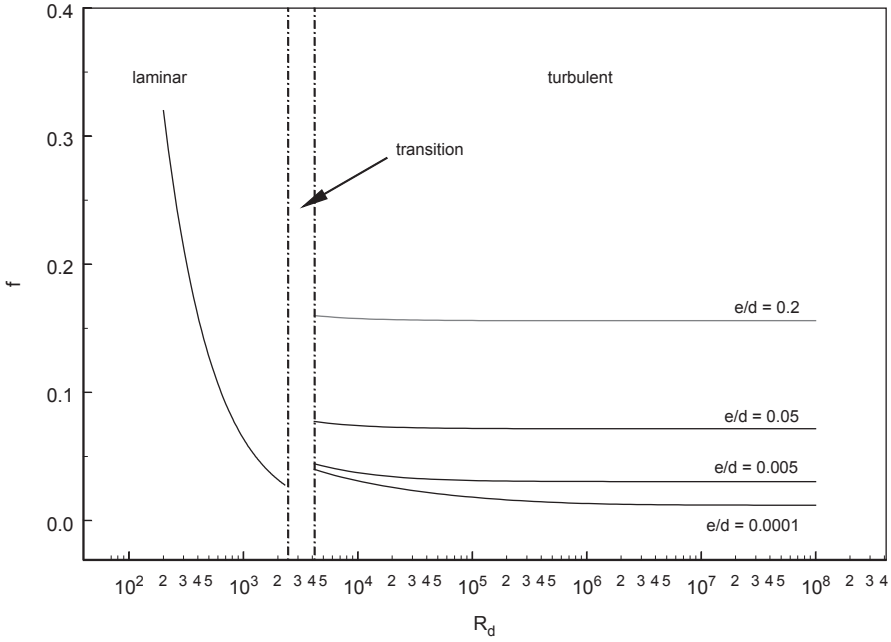


**Fig. 18.8** Friction factor

$$f = \begin{cases} \dfrac{64}{R_d}, & R_d \le 2300 \\ \dfrac{0.3086}{\log^2\left[\dfrac{6.9}{R_d} + \left(\dfrac{e}{3.7}\right)^{1.11}\right]}, & R_d \ge 4000 \end{cases} \tag{18.30}$$

The first result, due to Prandtl, may be found in many textbooks, for example, White (1986). The second equation was given by Haaland (1983).

## 18.5 System Characteristic

Consider the ventilation system diagrammed in Fig. 18.9. Let us suppose that we have estimated the pressure distribution around the car. We would now like to develop a composite loss coefficient for the system and use it to find the flow under the cruise condition and to size the fan so that we get at least the required minimum flow when the car is stopped.

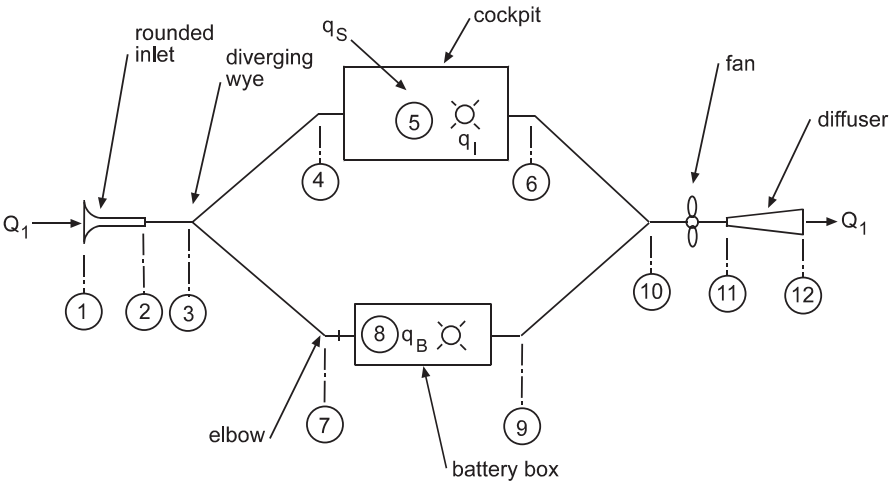


**Fig. 18.9** A ventilation system

The system has an inlet, a cockpit branch, and a battery branch, and then the ducts join and connect to the fan. The fan discharges through a diffuser to the external flow. Also shown are heat inputs to the cockpit from the sun ($q_s$, arrow) and from the driver and the instruments ($q_I$, rayed circle).

We will ignore the fan for now and discuss only the system external to it. Note that some of the components are in series with the flow so that the pressure drops to an additional amount as each component is traversed by the air. So the rule for series components is to add the pressure (or head) loss for each. The flow is the same through each series component, although the velocity may vary because of flow area changes. We can use Eq. (C.16) to convert the velocity to the volumetric flow. This can then be factored from the sum. For example, suppose the flow area of duct length $l_{2,3}$ is $A_3$ and the discharge area of the rounded inlet is $A_2$.

$$\Delta p_{2,3} = \frac{\rho K_{2,3}}{2A_3^2} Q_1^2 = k_{2,3} Q_1^2 \tag{18.31}$$

The lower case *k* represents a pressure loss coefficient, rather than a head loss coefficient, referenced to the entering flow.

But how about the parallel cockpit and battery branches? Proceeding in a fashion similar to the analysis of the divided flow around the car, we can develop an equivalent flow resistance, $k_{E_{3,10}}$ to represent the pressure loss of those two paths together.

$$\Delta p = k_{E_{3,10}} Q_1^2 = k_{U_{3,10}} Q_U^2 = k_{U_{3,10}} Q_L^2 \tag{18.32}$$

Substituting this into Eq. (18.7) gives

$$k_{E_{3,10}}^{-\frac{1}{2}} = k_{U_{3,10}}^{-\frac{1}{2}} + k_{L_{3,10}}^{-\frac{1}{2}} \tag{18.33}$$

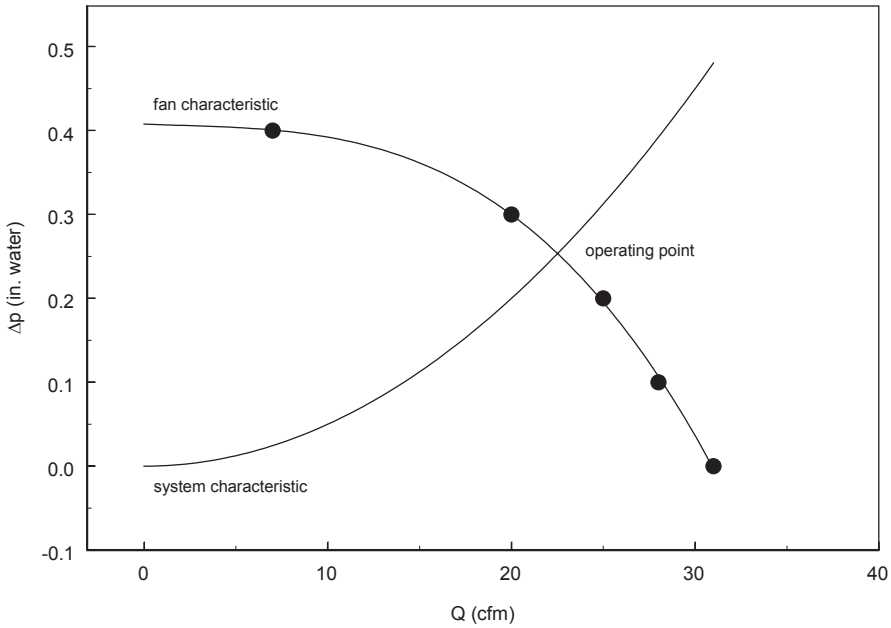


**Fig. 18.10** Fan and system characteristic

Where $k_{E_{3,10}}$ is the equivalent loss coefficient of the parallel branches and $k_{U_{3,10}}$ and $k_{L_{3,10}}$ are the series loss coefficients of the upper and lower branches, respectively. Now, the equivalent loss coefficient can be summed with the series loss coefficients for the components between stations 1 and 3 and stations 7 and 12.

$$k_S = k_{1,3} + k_{E_{3,10}} + k_{10,12} \tag{18.34}$$

The pressure loss for the system is

$$\Delta p = k_S Q_1^2 \tag{18.35}$$

This equation is plotted as the "system characteristic" in Fig. 18.10.

## 18.6 Fan

The purpose of the fan is to add energy to the air flow to offset the head losses. This head gain is a function of the flow rate and the rotational speed of the fan. We will consider herein a single-speed fan because this represents the usual case. Figure 18.10 shows a fan head-flow characteristic. The filled circles indicate that this curve must be obtained from the data furnished by the manufacturer. Note that the head produced is a function of the flow rate.

The intersection of the fan and system characteristics determines the flow through the system. This point usually must be calculated by trial-and-error, although it may be easily read from a graph (to within the scale) like Fig. 18.10.

## 18.7 Heating

*Design Heat Load* The rate of solar heating of the cockpit, plus the contribution of the instruments and the driver's body, is the load that must be used to design the cockpit's ventilation system. The radiation entering the cockpit causes negligible direct heating of the air through which it passes. However, surfaces in the cockpit absorb some of the radiation. This energy input tends to cause the temperatures of the absorbing surfaces to rise, thereby heating the air in contact with them. If the air flow through the cockpit cannot remove this energy at the rate it is absorbed, the temperatures in the cockpit will increase. Chap. 7 mentions that an air temperature of 120°F was measured in a solar racer cockpit when the racer was in slowly-moving traffic on a hot day in summer.

*Battery* The heat given off by the battery can be estimated with the knowledge of the battery's efficiency. For instance, suppose at the ventilation design condition, the battery was discharging at 120 V and 10 A, that is, at 1200 W. Then, if the discharge efficiency was 80 %, 240 W would have been dissipated in the process. The battery box air temperature is estimated by assuming that the walls of the box are essentially insulators and therefore all of the battery heat must be carried off by the air.

*Solar Gain* The fraction of the solar energy incident on the cockpit's glazing and absorbed in the cockpit surfaces is

$$\tau_c \alpha_{eff} = \tau_c \frac{\alpha_i}{\alpha_i + (1 - \alpha_i)\tau_d \dfrac{A_a}{A_i}} \tag{18.36}$$

(Duffie and Beckman 1991). Where $\tau_c$ is the transmittance of the glazing for the incident solar radiation, $\tau_d$ is the transmittance for isotropic diffuse solar radiation (calculate as for beam but with an effective angle of incidence of 60°), $A_a$ is the area of the cockpit's glazing, $A_i$ is the area of the surfaces inside of the cockpit (not including the glazing), and $\alpha_i$ is the mean absorbance for diffuse radiation of these inner surfaces.

Siegel (1973) presents a more elaborate model.

*Instruments* The heat dissipation of each instrument or cockpit light is equal to its operating power. For example, if an instrument requires 12 V at 1 mA, then it dissipates 12 mW of heat.

*Temperature* We will assume that the ventilation and heat flows are steady and that the air temperature is uniform across the inlet and outlet of the cockpit. Accounting for all energy flows gives $T_{outlet}$, the cockpit outlet temperature, as

$$T_{outlet} = \frac{\dot{Q}_{sun} + \dot{Q}_{inst} + \dot{Q}_{driver}}{\dot{m}c_P} + T_{inlet} \tag{18.37}$$

Where the symbol $\dot{Q}$ denotes the heat inputs previously discussed, $\dot{m}$ is the mass flow rate, $c_P$ now represents the specific heat at constant pressure of the entering air. This is a conservative calculation because it assumes that all the absorbed radiation will be transferred to the ventilation air.

## 18.8 Relative Humidity

The design environmental conditions should include a relative humidity and an air temperature. These should be assigned to the incoming ventilation air.

## References

ASHRAE. (1981). *Thermal environmental condition for human occupancy*. Atlanta: American Society of Heating, Refrigerating and Air-Conditioning Engineers, Inc.

Crane. (1969). *Flow of fluids through valves, fittings, and pipe*. Technical Paper no. 410. New York: Crane Company.

Haaland, S. E. (1983). Simple and explicit formulas for the friction factor in turbulent pipe flow. *Journal of Fluids Engineering, 105,* 89–90.

Idel'chik, I. E., (1966). *Handbook of hydraulic resistance coefficients of local resistance and of friction*, AEC-TR-6630, NTIS. Springfield: Virginia.

Siegel, R. (1973). Net radiation method for enclosure systems involving partially transparent walls, NASA TN D-7384, August

Wallis, S. B. (1971). Ventilation system aerodynamics–A new design method. SAE paper 710036, Automotive Engineering Congress, Detroit, Michigan, January 11–15, 1971.

White, F. M. (1986). *Fluid mechanics* (2nd ed.). New York: McGraw-Hill Book Company.